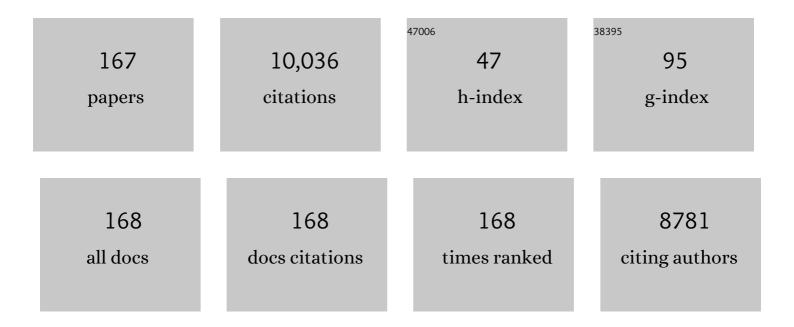
## Shiyu Du

List of Publications by Year in descending order

Source: https://exaly.com/author-pdf/816896/publications.pdf Version: 2024-02-01



#	Article	IF	CITATIONS
1	A general Lewis acidic etching route for preparing MXenes with enhanced electrochemical performance in non-aqueous electrolyte. Nature Materials, 2020, 19, 894-899.	27.5	870
2	Element Replacement Approach by Reaction with Lewis Acidic Molten Salts to Synthesize Nanolaminated MAX Phases and MXenes. Journal of the American Chemical Society, 2019, 141, 4730-4737.	13.7	811
3	Photoluminescent Ti <sub>3</sub> C <sub>2</sub> MXene Quantum Dots for Multicolor Cellular Imaging. Advanced Materials, 2017, 29, 1604847.	21.0	692
4	A Twoâ€Dimensional Zirconium Carbide by Selective Etching of Al <sub>3</sub> C <sub>3</sub> from Nanolaminated Zr <sub>3</sub> Al <sub>3</sub> C <sub>5</sub> . Angewandte Chemie - International Edition, 2016, 55, 5008-5013.	13.8	425
5	Synthesis and Electrochemical Properties of Two-Dimensional Hafnium Carbide. ACS Nano, 2017, 11, 3841-3850.	14.6	370
6	Role of the surface effect on the structural, electronic and mechanical properties of the carbide MXenes. Europhysics Letters, 2015, 111, 26007.	2.0	262
7	Enhanced thermal properties of poly(vinylidene fluoride) composites with ultrathin nanosheets of MXene. RSC Advances, 2017, 7, 20494-20501.	3.6	242
8	Rational Design of Flexible Two-Dimensional MXenes with Multiple Functionalities. Chemical Reviews, 2019, 119, 11980-12031.	47.7	242
9	Loading Actinides in Multilayered Structures for Nuclear Waste Treatment: The First Case Study of Uranium Capture with Vanadium Carbide MXene. ACS Applied Materials & Interfaces, 2016, 8, 16396-16403.	8.0	214
10	Metal-Level Thermally Conductive yet Soft Graphene Thermal Interface Materials. ACS Nano, 2019, 13, 11561-11571.	14.6	214
11	Facile preparation of in situ coated Ti <sub>3</sub> C <sub>2</sub> T <sub>x</sub> /Ni <sub>0.5</sub> Zn <sub>0.5</sub> Fe <sub>2</sub> O <sub>4&lt; and their electromagnetic performance. RSC Advances, 2017, 7, 24698-24708.</sub>	/sabs>com	ip <b>æsite</b> s
12	Promising electron mobility and high thermal conductivity in Sc <sub>2</sub> CT <sub>2</sub> (T = F,) Tj ETQq0 (	) 0.rgBT /0	Overlock 10 T
13	Halogenated Ti <sub>3</sub> C <sub>2</sub> MXenes with Electrochemically Active Terminals for High-Performance Zinc Ion Batteries. ACS Nano, 2021, 15, 1077-1085.	14.6	183
14	The thermal and electrical properties of the promising semiconductor MXene Hf2CO2. Scientific Reports, 2016, 6, 27971.	3.3	178
15	In situ formation of a cellular graphene framework in thermoplastic composites leading to superior thermal conductivity. Journal of Materials Chemistry A, 2017, 5, 6164-6169.	10.3	149
16	Intrinsic Structural, Electrical, Thermal, and Mechanical Properties of the Promising Conductor Mo <sub>2</sub> C MXene. Journal of Physical Chemistry C, 2016, 120, 15082-15088.	3.1	139
17	Rational Design of Highly Stable and Active MXeneâ€Based Bifunctional ORR/OER Doubleâ€Atom Catalysts. Advanced Materials, 2021, 33, e2102595.	21.0	137
18	A Paper-Like Inorganic Thermal Interface Material Composed of Hierarchically Structured	14.6	131

Graphene/Silicon Carbide Nanorods. ACS Nano, 2019, 13, 1547-1554. ·) 14.6 131

Sніти Du

#	Article	IF	CITATIONS
19	The critical issues of SiC materials for future nuclear systems. Scripta Materialia, 2018, 143, 149-153.	5.2	127
20	Rare earth separations by selective borate crystallization. Nature Communications, 2017, 8, 14438.	12.8	125
21	High-Resolution Dynamic Pressure Sensor Array Based on Piezo-phototronic Effect Tuned Photoluminescence Imaging. ACS Nano, 2015, 9, 3143-3150.	14.6	122
22	Exceptionally high thermal and electrical conductivity of three-dimensional graphene-foam-based polymer composites. RSC Advances, 2016, 6, 22364-22369.	3.6	105
23	Graphene foam-embedded epoxy composites with significant thermal conductivity enhancement. Nanoscale, 2019, 11, 17600-17606.	5.6	105
24	Strong and biocompatible poly(lactic acid) membrane enhanced by Ti3C2Tz (MXene) nanosheets for Guided bone regeneration. Materials Letters, 2018, 229, 114-117.	2.6	100
25	Direct in situ observation and explanation of lithium dendrite of commercial graphite electrodes. RSC Advances, 2015, 5, 69514-69521.	3.6	93
26	Lattice Matching and Halogen Regulation for Synergistically Induced Uniform Zinc Electrodeposition by Halogenated Ti <sub>3</sub> C <sub>2</sub> MXenes. ACS Nano, 2022, 16, 813-822.	14.6	90
27	Novel Scaleâ€Like Structures of Graphite/TiC/Ti <sub>3</sub> C <sub>2</sub> Hybrids for Electromagnetic Absorption. Advanced Electronic Materials, 2018, 4, 1700617.	5.1	86
28	Multielemental single–atom-thick <i>A</i> layers in nanolaminated V <sub>2</sub> (Sn, <i>A</i> ) C () Tj ETQ Sciences of the United States of America, 2020, 117, 820-825.	q0 0 0 rgB 7.1	T /Overlock 1 84
29	Ti <sub>n+1</sub> C <sub>n</sub> MXenes with fully saturated and thermally stable Cl terminations. Nanoscale Advances, 2019, 1, 3680-3685.	4.6	81
30	Superlubricity Enabled by Pressure-Induced Friction Collapse. Journal of Physical Chemistry Letters, 2018, 9, 2554-2559.	4.6	79
31	Cytocompatibility of Ti <sub>3</sub> AlC <sub>2</sub> , Ti <sub>3</sub> SiC <sub>2</sub> , and Ti <sub>2</sub> AlN: <i>In Vitro</i> Tests and First-Principles Calculations. ACS Biomaterials Science and Engineering, 2017, 3, 2293-2301.	5.2	75
32	How Does the Hydrogen Bonding Interaction Influence the Properties of Polybenzoxazine? An Experimental Study Combined with Computer Simulation. Macromolecules, 2018, 51, 4782-4799.	4.8	75
33	Metal–Semiconductor Phase Twinned Hierarchical MoS <sub>2</sub> Nanowires with Expanded Interlayers for Sodiumâ€ion Batteries with Ultralong Cycle Life. Small, 2020, 16, e1906607.	10.0	74
34	VFFDT: A New Software for Preparing AMBER Force Field Parameters for Metal-Containing Molecular Systems. Journal of Chemical Information and Modeling, 2016, 56, 811-818.	5.4	73
35	Structures and Mechanical and Electronic Properties of the Ti2CO2 MXene Incorporated with Neighboring Elements (Sc, V, B and N). Journal of Electronic Materials, 2017, 46, 2460-2466.	2.2	68
36	The OH radical-H2O molecular interaction potential. Journal of Chemical Physics, 2006, 124, 224318.	3.0	67

#	Article	IF	CITATIONS
37	A Twoâ€Dimensional Zirconium Carbide by Selective Etching of Al <sub>3</sub> C <sub>3</sub> from Nanolaminated Zr <sub>3</sub> Al <sub>3</sub> C <sub>5</sub> . Angewandte Chemie, 2016, 128, 5092-5097.	2.0	65
38	First-principles investigations on the electronic structures of U3Si2. Journal of Nuclear Materials, 2016, 469, 194-199.	2.7	65
39	Effect of carbide interlayers on the microstructure and properties of graphene-nanoplatelet-reinforced copper matrix composites. Materials Science & Engineering A: Structural Materials: Properties, Microstructure and Processing, 2017, 708, 311-318.	5.6	65
40	Fast joining SiC ceramics with Ti3SiC2 tape film by electric field-assisted sintering technology. Journal of Nuclear Materials, 2015, 466, 322-327.	2.7	64
41	Coordination Polymer-Derived Multishelled Mixed Ni–Co Oxide Microspheres for Robust and Selective Detection of Xylene. ACS Applied Materials & Interfaces, 2018, 10, 15314-15321.	8.0	64
42	Encapsulation kinetics and dynamics of carbon monoxide in clathrate hydrate. Nature Communications, 2014, 5, 4128.	12.8	62
43	Single-Atom-Thick Active Layers Realized in Nanolaminated Ti <sub>3</sub> (Al <sub><i>x</i></sub> Cu <sub>1–<i>x</i></sub> )C <sub>2</sub> and Its Artificial Enzyme Behavior. ACS Nano, 2019, 13, 9198-9205.	14.6	59
44	Thickness-dependent phase evolution and bonding strength of SiC ceramics joints with active Ti interlayer. Journal of the European Ceramic Society, 2017, 37, 1233-1241.	5.7	58
45	Synthesis of MAX phases Nb <sub>2</sub> CuC and Ti <sub>2</sub> (Al <sub>0.1</sub> Cu <sub>0.9</sub> )N by A-site replacement reaction in molten salts. Materials Research Letters, 2019, 7, 510-516.	8.7	58
46	Lightweight thermal interface materials based on hierarchically structured graphene paper with superior through-plane thermal conductivity. Chemical Engineering Journal, 2021, 419, 129609.	12.7	54
47	Enhanced Electromagnetic Shielding and Thermal Conductive Properties of Polyolefin Composites with a Ti <sub>3</sub> C <sub>2</sub> T <sub><i>x</i></sub> MXene/Graphene Framework Connected by a Hydrogen-Bonded Interface. ACS Nano, 2022, 16, 9254-9266.	14.6	54
48	Designing flexible 2D transition metal carbides with strain-controllable lithium storage. Proceedings of the National Academy of Sciences of the United States of America, 2017, 114, E11082-E11091.	7.1	51
49	Tuning the Electrical Conductivity of Ti <sub>2</sub> CO <sub>2</sub> MXene by Varying the Layer Thickness and Applying Strains. Journal of Physical Chemistry C, 2019, 123, 6802-6811.	3.1	49
50	Electronic and Transport Properties of Ti <sub>2</sub> CO <sub>2</sub> MXene Nanoribbons. Journal of Physical Chemistry C, 2016, 120, 17143-17152.	3.1	46
51	Mechanism of Al on FeCrAl steam oxidation behavior and molecular dynamics simulations. Journal of Alloys and Compounds, 2020, 828, 154310.	5.5	44
52	Fabrication of Ti 2 AlN ceramics with orientation growth behavior by the microwave sintering method. Journal of the European Ceramic Society, 2015, 35, 1385-1391.	5.7	42
53	Templateâ€Free Growth of Wellâ€Ordered Silver Nano Forest/Ceramic Metamaterial Films with Tunable Optical Responses. Advanced Materials, 2017, 29, 1605324.	21.0	42
54	Single Atomâ€Modified Hybrid Transition Metal Carbides as Efficient Hydrogen Evolution Reaction Catalysts. Advanced Functional Materials, 2021, 31, 2104285.	14.9	42

Sніyu Du

#	Article	IF	CITATIONS
55	Manganese-Zeolitic Imidazolate Frameworks-90 with High Blood Circulation Stability for MRI-Guided Tumor Therapy. Nano-Micro Letters, 2019, 11, 61.	27.0	40
56	Highly Conductive 3D Segregated Graphene Architecture in Polypropylene Composite with Efficient EMI Shielding. Polymers, 2017, 9, 662.	4.5	38
57	Synthesis and properties of conductive B <sub>4</sub> C ceramic composites with TiB <sub>2</sub> grain network. Journal of the American Ceramic Society, 2018, 101, 3780-3786.	3.8	38
58	Two-Dimensional Lamellar Mo <sub>2</sub> C for Electrochemical Hydrogen Production: Insights into the Origin of Hydrogen Evolution Reaction Activity in Acidic and Alkaline Electrolytes. ACS Applied Materials & Interfaces, 2018, 10, 40500-40508.	8.0	38
59	Mo <sub>2</sub> B, an MBene member with high electrical and thermal conductivities, and satisfactory performances in lithium ion batteries. Nanoscale Advances, 2020, 2, 347-355.	4.6	38
60	Crystal structure and encapsulation dynamics of ice II-structured neon hydrate. Proceedings of the National Academy of Sciences of the United States of America, 2014, 111, 10456-10461.	7.1	36
61	Controllable magnitude and anisotropy of the electrical conductivity of Hf <sub>3</sub> C <sub>2</sub> O <sub>2</sub> MXene. Journal of Physics Condensed Matter, 2017, 29, 165701.	1.8	35
62	Negative differential resistance and rectifying performance induced by doped graphene nanoribbons p – n device. Physics Letters, Section A: General, Atomic and Solid State Physics, 2016, 380, 1049-1055.	2.1	34
63	Surface Electrochemical Stability and Strainâ€Tunable Lithium Storage of Highly Flexible 2D Transition Metal Carbides. Advanced Functional Materials, 2018, 28, 1804867.	14.9	33
64	MAX phase Zr2SeC and its thermal conduction behavior. Journal of the European Ceramic Society, 2021, 41, 4447-4451.	5.7	33
65	Pancake ï€â€"ï€ Bonding Goes Double: Unexpected 4e/All-Sites Bonding in Boron- and Nitrogen-Doped Phenalenyls. Journal of Physical Chemistry Letters, 2015, 6, 2318-2325.	4.6	32
66	Facile and Efficient Decontamination of Thorium from Rare Earths Based on Selective Selenite Crystallization. Inorganic Chemistry, 2018, 57, 1880-1887.	4.0	32
67	Exploring the potential of exfoliated ternary ultrathin Ti <sub>4</sub> AlN <sub>3</sub> nanosheets for fabricating hybrid patterned polymer brushes. RSC Advances, 2015, 5, 70339-70344.	3.6	30
68	The development of cladding materials for the accident tolerant fuel system from the Materials Genome Initiative. Scripta Materialia, 2017, 141, 99-106.	5.2	30
69	Two-Dimensional Hydroxyl-Functionalized and Carbon-Deficient Scandium Carbide, ScC <sub><i>x</i></sub> OH, a Direct Band Gap Semiconductor. ACS Nano, 2019, 13, 1195-1203.	14.6	30
70	Two-dimensional semiconducting Lu <sub>2</sub> CT <sub>2</sub> (T = F, OH) MXene with low work function and high carrier mobility. Nanoscale, 2020, 12, 3795-3802.	5.6	30
71	Mechanistic Quantification of Thermodynamic Stability and Mechanical Strength for Two-Dimensional Transition-Metal Carbides. Journal of Physical Chemistry C, 2018, 122, 4710-4722.	3.1	28
72	Bipolar magnetic semiconductors among intermediate states during the conversion from Sc <sub>2</sub> C(OH) <sub>2</sub> to Sc <sub>2</sub> CO <sub>2</sub> MXene. Nanoscale, 2018, 10, 8763-8771.	5.6	27

Sніуи Du

#	Article	IF	CITATIONS
73	Theory-guided bottom-up design of the FeCrAl alloys as accident tolerant fuel cladding materials. Journal of Nuclear Materials, 2019, 516, 63-72.	2.7	27
74	New insight into the helium-induced damage in MAX phase Ti3AlC2 by first-principles studies. Journal of Chemical Physics, 2015, 143, 114707.	3.0	26
75	First-principles study of the electronic, optical and transport of few-layer semiconducting MXene. Computational Materials Science, 2019, 168, 137-143.	3.0	26
76	Hierarchical Co3O4@NiMoO4 core-shell nanowires for chemiresistive sensing of xylene vapor. Mikrochimica Acta, 2019, 186, 222.	5.0	26
77	Boosting Oxygen Reduction for Highâ€Efficiency H <sub>2</sub> O <sub>2</sub> Electrosynthesis on Oxygen oordinated CoNC Catalysts. Small, 2022, 18, e2200730.	10.0	25
78	Interaction between OH Radical and the Water Interface. Journal of Physical Chemistry A, 2008, 112, 4826-4835.	2.5	24
79	Uranyl Carboxyphosphonates Derived from Hydrothermal in Situ Ligand Reaction: Syntheses, Structures, and Computational Investigations. Inorganic Chemistry, 2015, 54, 8617-8624.	4.0	24
80	First-principles study on the electrical and thermal properties of the semiconducting Sc <sub>3</sub> (CN)F <sub>2</sub> MXene. RSC Advances, 2018, 8, 22452-22459.	3.6	24
81	Mg@C60 nano-lamellae and its 12.50Âwt% hydrogen storage capacity. International Journal of Hydrogen Energy, 2019, 44, 15239-15245.	7.1	24
82	Preparation of TiC/Ti <sub>2</sub> AlC coating on carbon fiber and investigation of the oxidation resistance properties. Journal of the American Ceramic Society, 2018, 101, 5269-5280.	3.8	23
83	Electrochemical Lithium Storage Performance of Molten Salt Derived V2SnC MAX Phase. Nano-Micro Letters, 2021, 13, 158.	27.0	23
84	Determination of the rate constant for sulfur recombination by quasiclassical trajectory calculations. Journal of Chemical Physics, 2008, 128, 204306.	3.0	22
85	Development of interatomic potentials for Fe-Cr-Al alloy with the particle swarm optimization method. Journal of Alloys and Compounds, 2019, 780, 881-887.	5.5	22
86	The role of Hume-Rothery's rules play in the MAX phases formability. Materialia, 2020, 12, 100810.	2.7	22
87	High Pressure Phase-Transformation Induced Texture Evolution and Strengthening in Zirconium Metal: Experiment and Modeling. Scientific Reports, 2015, 5, 12552.	3.3	21
88	Electronic structures and mechanical properties of Al(111)/ZrB <sub>2</sub> (0001) heterojunctions from first-principles calculation. Molecular Physics, 2015, 113, 1794-1801.	1.7	21
89	Interaction of CIO Radical with Liquid Water. Journal of the American Chemical Society, 2009, 131, 14778-14785.	13.7	20
90	Label-Free Electrochemical Detection of Vanillin through Low-Defect Graphene Electrodes Modified with Au Nanoparticles. Materials, 2018, 11, 489.	2.9	20

#	Article	IF	CITATIONS
91	Study of electronic structure and dynamics of interacting free radicals influenced by water. Journal of Chemical Physics, 2009, 130, 124312.	3.0	19
92	Effects of Different Surface Functionalization and Doping on the Electronic Transport Properties of M <sub>2</sub> CT <i><sub>x</sub></i> –M <sub>2</sub> CO <sub>2</sub> Heterojunction Devices. Journal of Physical Chemistry C, 2018, 122, 14908-14917.	3.1	18
93	Structural, mechanical and electronic properties of two-dimensional chlorine-terminated transition metal carbides and nitrides. Journal of Physics Condensed Matter, 2020, 32, 135302.	1.8	18
94	Theoretical investigations on helium trapping in the Zr/Ti 2 AlC interface. Surface and Coatings Technology, 2017, 322, 19-24.	4.8	17
95	Residual thermal stress of SiC/Ti <sub>3</sub> SiC <sub>2</sub> /SiC joints calculation and relaxed by postannealing. International Journal of Applied Ceramic Technology, 2018, 15, 1157-1165.	2.1	17
96	Highly Sensitive and Selective Potassium Ion Detection Based on Graphene Hall Effect Biosensors. Materials, 2018, 11, 399.	2.9	17
97	Surface Modification Using Polydopamine-Coated Liquid Metal Nanocapsules for Improving Performance of Graphene Paper-Based Thermal Interface Materials. Nanomaterials, 2021, 11, 1236.	4.1	17
98	Ab Initio Studies on the Clathrate Hydrates of Some Nitrogen- and Sulfur-Containing Gases. Journal of Physical Chemistry A, 2017, 121, 2620-2626.	2.5	16
99	High Oxidation Resistance of CVD Graphene-Reinforced Copper Matrix Composites. Nanomaterials, 2019, 9, 498.	4.1	16
100	Rational design of high-performance thermal interface materials based on gold-nanocap-modified vertically aligned graphene architecture. Composites Communications, 2021, 24, 100621.	6.3	16
101	Current rectification induced by V-doped and Sc-doped in Ti2CO2 devices. Computational Materials Science, 2017, 138, 175-182.	3.0	15
102	Layer-by-layer stacked graphene nanocoatings by Marangoni self-assembly for corrosion protection of stainless steel. Chinese Chemical Letters, 2021, 32, 501-505.	9.0	15
103	Molten Salt Synthesis of Nanolaminated Sc <sub>2</sub> SnC MAX Phase. Wuji Cailiao Xuebao/Journal of Inorganic Materials, 2021, 36, 773.	1.3	15
104	Y1 receptor ligand-based nanomicelle as a novel nanoprobe for glioma-targeted imaging and therapy. Nanoscale, 2018, 10, 5845-5851.	5.6	14
105	Copper–SiC whiskers composites with interface optimized by Ti3SiC2. Journal of Materials Science, 2018, 53, 9806-9815.	3.7	14
106	Facilitating effect of heavy metals on di(2-ethylhexyl) phthalate adsorption in soil: New evidence from adsorption experiment data and quantum chemical simulation. Science of the Total Environment, 2021, 772, 144980.	8.0	14
107	Near-room temperature ferromagnetic behavior of single-atom-thick 2D iron in nanolaminated ternary MAX phases. Applied Physics Reviews, 2021, 8, .	11.3	14
108	Many-body decomposition of the binding energies for OHâ‹(H2O)2 and OHâ‹(H2O)3 complexes. Journal of Chemical Physics, 2008, 128, 084307.	3.0	13

#	Article	IF	CITATIONS
109	How Vertical Compression Triggers Lateral Interlayer Slide for Metallic Molybdenum Disulfide?. Tribology Letters, 2018, 66, 1.	2.6	13
110	Grand Canonical Monte Carlo Simulations on Phase Equilibria of Methane, Carbon Dioxide, and Their Mixture Hydrates. Journal of Physical Chemistry B, 2018, 122, 9724-9737.	2.6	13
111	Mutual Identification between the Pressure-Induced Superlubricity and the Image Contrast Inversion of Carbon Nanostructures from AFM Technology. Journal of Physical Chemistry Letters, 2019, 10, 1498-1504.	4.6	13
112	Interface modification of carbon fibers with TiC/Ti2AlC coating and its effect on the tensile strength. Ceramics International, 2019, 45, 4661-4666.	4.8	13
113	ZnO nanoflowers modified with RuO2 for enhancing acetone sensing performance. Nanotechnology, 2020, 31, 115502.	2.6	13
114	Theoretical study on the electrical and mechanical properties of MXene multilayer structures through strain regulation. Chemical Physics Letters, 2020, 760, 137997.	2.6	13
115	Two-Dimensional Carbonitride MXenes as an Efficient Electrocatalyst for Hydrogen Evolution. Journal of Physical Chemistry C, 2021, 125, 4477-4488.	3.1	13
116	Structures and Mechanical Properties of CH <sub>4</sub> , SO <sub>2</sub> , and H <sub>2</sub> S Hydrates from Density Function Theory Calculations. Chemistry Letters, 2017, 46, 1141-1144.	1.3	12
117	Reprint of: The development of cladding materials for the accident tolerant fuel system from the Materials Genome Initiative. Scripta Materialia, 2018, 143, 129-136.	5.2	12
118	Non-MAX Phase Precursors for MXenes. , 2019, , 53-68.		12
119	Ab initio and analytical intermolecular potential for ClO–H2O. Journal of Chemical Physics, 2007, 126, 114304.	3.0	11
120	Spectroscopic properties and stability of the SHâ‹H2O open shell complex. Journal of Chemical Physics, 2009, 130, 124304.	3.0	11
121	Improved lysis of single bacterial cells by a modified alkaline-thermal shock procedure. BioTechniques, 2016, 60, 129-135.	1.8	11
122	A theoretical investigation and synthesis of layered ternary carbide system U-Al-C. Ceramics International, 2018, 44, 1646-1652.	4.8	11
123	The compositional dependence of structural stability and resulting properties for Mn+1CnT2 (M = Sc,) Tj ETQq1 Technology, 2020, 9, 14979-14989.	1 0.78431 5.8	4 rgBT /Ove 11
124	First-principles investigations on MXene-blue phosphorene and MXene-MoS2 transistors. Nanotechnology, 2020, 31, 395203.	2.6	11
125	Pt nanodendrites with (111) crystalline facet as an efficient, stable and pH-universal catalyst for electrochemical hydrogen production. Chinese Chemical Letters, 2020, 31, 2478-2482.	9.0	11
126	First-principles study of magnetism in some novel MXene materials. RSC Advances, 2020, 10, 44430-44436.	3.6	11

#	Article	IF	CITATIONS
127	Structural, electronic and mechanical properties of (NbxTi1â^'x)2SC and (NbxZr1â^'x)2SC (0⩽x⩽1) from first-principles investigations. Computational and Theoretical Chemistry, 2016, 1090, 58-66.	2.5	10
128	Adsorption Behaviors and Phase Equilibria for Clathrate Hydrates of Sulfur- and Nitrogen-Containing Small Molecules. Journal of Physical Chemistry C, 2019, 123, 2691-2702.	3.1	10
129	Theoretical exploration on the vibrational and mechanical properties of M <sub>3</sub> C <sub>2</sub> /M <sub>3</sub> C <sub>2</sub> T <sub>2</sub> MXenes. International Journal of Quantum Chemistry, 2020, 120, e26409.	2.0	10
130	Electric Field Effect on the Reactivity of Solid State Materials: The Case of Single Layer Graphene. Advanced Functional Materials, 2020, 30, 1909269.	14.9	10
131	A synergetic stabilization and strengthening strategy for two-dimensional ordered hybrid transition metal carbides. Physical Chemistry Chemical Physics, 2018, 20, 29684-29692.	2.8	9
132	First-principles investigations on the anisotropic elasticity and thermodynamic properties of U <sub>3</sub> Si <sub>2</sub> –Al. RSC Advances, 2020, 10, 35049-35056.	3.6	9
133	Phonon-mediated stabilization and softening of 2D transition metal carbides: case studies of Ti <sub>2</sub> CO <sub>2</sub> and Mo <sub>2</sub> CO <sub>2</sub> . Physical Chemistry Chemical Physics, 2018, 20, 14608-14618.	2.8	8
134	OH â‹ N 2 and SHâ‹N2 radical-molecule van der Waals complex. Journal of Chemical Physics, 2009, 131, 064307.	3.0	7
135	Hybridization of inorganic CoB noncrystal with graphene and its Kubas-enhanced hydrogen adsorption at room temperature. RSC Advances, 2016, 6, 93238-93244.	3.6	7
136	Abnormal grain growth of UO2 with pores in the final stage of sintering: A phase field study. Computational Materials Science, 2018, 145, 24-34.	3.0	7
137	Theoretical investigations on structural and thermo-mechanical properties of layered ternary carbide Th–Al–C systems. Journal of Nuclear Materials, 2020, 540, 152358.	2.7	7
138	Investigations of the stability and electronic structures of U3Si2-Al: A first-principles study. Chemical Physics, 2021, 543, 111088.	1.9	7
139	A Novel Chimp Optimization Algorithm with Refraction Learning and Its Engineering Applications. Algorithms, 2022, 15, 189.	2.1	7
140	3D Graphene Oxide Micropatterns Achieved by Rollerâ€Assisted Microcontact Printing Induced Interface Integral Peel and Transfer. Advanced Materials Interfaces, 2017, 4, 1600867.	3.7	6
141	Electronic structures, mechanical properties and defect formation energies of U3Si5 from density functional theory calculations. Progress in Nuclear Energy, 2019, 116, 87-94.	2.9	6
142	Defective structures in FeCrAl alloys from first principles calculations. Japanese Journal of Applied Physics, 2020, 59, 046003.	1.5	6
143	A dense graphene monolith with poloxamer prefunctionalization enabling aqueous redispersion to obtain solubilized graphene sheets. Chinese Chemical Letters, 2020, 31, 2507-2511.	9.0	6
144	Chalcogenide MAX phases Zr2Se(B1-xSex) (x=0–0.97) and their conduction behaviors. Acta Materialia, 2022, 237, 118183.	7.9	6

Sніуи Du

#	Article	IF	CITATIONS
145	Universal Principle for Large-Scale Production of a High-Quality Two-Dimensional Monolayer via Positive Charge-Driven Exfoliation. Journal of Physical Chemistry Letters, 2022, 13, 6597-6603.	4.6	6
146	New formulation for reduction potentials of (Cu, Ni, Al, Zn)–lanthanide alloys – Implications for electrolysis-based pyroprocessing of spent nuclear fuel. Electrochemistry Communications, 2018, 93, 180-182.	4.7	5
147	First-principles study on the stability and properties of β-SiC/M+1AlC (M=Sc, Ti, V, Cr, Zr, Nb, Mo, Hf, Ta;) Tj ETQq	1 1 0.784 4.0	314 rgBT /0
148	First-principles investigations on the electronic structures, polycrystalline elastic properties, ideal strengths and elastic anisotropy of U3Si2. European Physical Journal Plus, 2021, 136, 1.	2.6	5
149	Revisiting alpha decay-based near-light-speed particle propulsion. Applied Radiation and Isotopes, 2016, 114, 14-18.	1.5	4
150	Designing Flexible Quantum Spin Hall Insulators through 2D Ordered Hybrid Transition-Metal Carbides. Journal of Physical Chemistry C, 2019, 123, 20664-20674.	3.1	4
151	The studies of electronic structure, mechanical properties and ideal fracture behavior of U3Si1.75Al0.25: first-principle investigations. Journal of Materials Research and Technology, 2021, 15, 1356-1369.	5.8	4
152	Role of the A-Element in the Structural, Mechanical, and Electronic Properties of Ti <sub>3</sub> AC <sub>2</sub> MAX Phases. Inorganic Chemistry, 2022, 61, 2129-2140.	4.0	4
153	Influence of passivation pretreatment in common acid and alkali on oxidation behaviour of Ti <sub>3</sub> SiC <sub>2</sub> at 500°C. Advances in Applied Ceramics, 2016, 115, 60-64.	1.1	3
154	Effect of electric current on diffusion of aluminum in Ti3AlC2 into zirconium alloy. Journal Wuhan University of Technology, Materials Science Edition, 2017, 32, 645-649.	1.0	3
155	A Study on the Periodic Rule of Reduction Potentials of Lanthanides on Liquid Zinc Electrode. Journal of the Electrochemical Society, 2019, 166, D689-D693.	2.9	3
156	Irradiation behavior of Cf/SiC composite with titanium carbide (TiC)-based interphase. Journal of Nuclear Materials, 2019, 523, 10-15.	2.7	3
157	Amorphous carbon to graphene: Carbon diffusion via nickel catalyst. Materials Letters, 2020, 278, 128468.	2.6	3
158	Theoretical studies on microstructures, stabilities and formation conditions of some sour gas in the type I, II, and H clathrate hydrates. Journal of Molecular Structure, 2018, 1153, 292-298.	3.6	2
159	Predictions of the structures and properties of the substituted layered ternary compound series (Zr1â´`x T x )3Al3C5 (T  =  Hf, Nb, and V) through first-principles studies. Journal of Physics Con Matter, 2019, 31, 385702.	dersed	2
160	MoO <sub><i>x</i></sub> Nanoparticle Catalysts for <scp>d</scp> -Glucose Epimerization and Their Electrical Immobilization in a Continuous Flow Reactor. ACS Applied Materials & Interfaces, 2019, 11, 44118-44123.	8.0	2
161	Theoretical investigations on the U2Mo3Si4 compound from first-principles calculations. Progress in Nuclear Energy, 2020, 118, 103121.	2.9	2
162	A damage-effect-involved phenomenological crystal plasticity model and computational methods for mechanical responses of FeCrAl alloys. Materials Today Communications, 2021, 28, 102595.	1.9	2

Sніүи Du

#	Article	IF	CITATIONS
163	Effect of Aâ€site atom on static corrosion behavior and irradiation damage of Ti <sub>2</sub> SC phases. Journal of the American Ceramic Society, 2022, 105, 1386-1393.	3.8	2
164	Development of a Phase Field Tool Coupling With Thermodynamic Data for Microstructure Evolution Simulation of Alloys in Nuclear Reactors. Frontiers in Materials, 2021, 8, .	2.4	1
165	The role of nuclear charges in unifying the descriptions of neural networks (NN)-based force fields. Materials Letters, 2020, 276, 128262.	2.6	0
166	Helium-induced damage in U3Si5 by first-principles studies. RSC Advances, 2021, 11, 26920-26927.	3.6	0
167	Pressure Tuned Structural, Electronic and Elastic Properties of U3Si2C2: A First Principles Study. Crystals, 2021, 11, 1420.	2.2	0